JOURNAL OF MAGNETIC RESONANCE **124,** 250–254 (1997)
ARTICLE NO. MN961049

Broadband Adiabatic Refocusing without Phase Distortion

TSANG-LIN HWANG,* PETER C. M. VAN ZIJL,* AND MICHAEL GARWOOD†

*Department of Radiology and Biophysics and Biophysical Chemistry, Johns Hopkins University School of Medicine, 217 Traylor Building, 720 Rutland Avenue, Baltimore, Maryland 21205; and †Center for Magnetic Resonance Research and Department of Radiology, University of Minnesota Medical School, Minneapolis, Minnesota 55455

Received October 24, 1996

Adiabatic pulses (*1–5*) can provide increased bandwidths and accurate flip angles, with high tolerance to spatial variations in RF field intensity. After being successfully applied to many aspects of *in vivo* surface coil NMR spectroscopy in the past decade, these pulses have recently gained popularity in high-resolution NMR for broadband decoupling (*6–8*) and for sensitivity enhancement, while simultaneously reducing artifacts (*9*) and permitting automation of complex pulse sequences (*10*). Because of the importance of low-power, broadband heteronuclear decoupling at high magnetic fields, much of the work has focused on the inversion properties of adiabatic full-passage (AFP) pulses.

However, an AFP pulse is not a suitable refocusing element in spin-echo sequences, since the pulse produces an undesirable phase roll across the spectrum as a function of chemical shift (*11, 12*). One approach to eliminate this problem relies on the formation of even-numbered echoes (e.g., a double-echo experiment) using identical 180° pulses which compensate the phase shifts created by one another (*13–15*). Other approaches for adiabatic refocusing use numerical and experimental pulse-shape optimizations of AFP pulses, such as CHIRP (*16*) and others (*17*). A final approach is based on the creation of composite adiabatic pulses, which contain inversions of the effective field B_{eff}. These ''B_{eff} flips'' (*3, 4, 11, 18*) reverse the direction of spin precession and compensate the phase shifts created in the separate adiabatic segments of the pulse. The so-called B_1-insensitive-rotation (BIR) pulses (*4*) are an example of this type of pulse. Like a conventional pulse, however, the bandwidth of current BIR pulses is limited by the available B_1 amplitude ($B_1^{\max}$). In this Communication, we demonstrate the potential to achieve unlimited bandwidths and excellent phase stability with a class of time-symmetric adiabatic refocusing pulses constructed from a series of AFP pulses separated by B_{eff} flips (*19*).

The description of these broadband adiabatic refocusing pulses can be facilitated by first examining the origin of the spectral phase roll produced by an AFP pulse when it is used as a refocusing element (*11*). This phenomenon can be understood by considering the motion of the transverse magnetization $\mathbf{M}$ in the appropriate rotating frames of reference. In most descriptions of conventional (constant frequency) pulses, the reference frame rotates at the carrier frequency ω_c, which is typically set to the Larmor frequency ω_0 at the center of the spectral region of interest. In this constant-frequency frame, a resonance offset ($\Omega = \omega_0 - \omega_c$) gives rise to a constant longitudinal field component of magnitude Ω/γ. A frequency-swept pulse, such as an AFP pulse, is most often described in the so-called frequency-modulated (FM) frame (1), which rotates at the time-dependent frequency of the pulse, $\omega(t)$. In the FM frame (Fig. 1a), with axes labeled x', y', z', the longitudinal field component is

$$\Delta\boldsymbol{\omega}(t) = [\omega_0 - \omega(t)]\hat{\mathbf{z}}' = [\Omega - AF_2(t)]\hat{\mathbf{z}}', \qquad [1]$$

where A is the amplitude of the frequency sweep (relative to ω_c) and $F_2(t)$ is a dimensionless function describing the frequency modulation with values in the range -1 to 1. In the FM frame, the effective magnetic field $\mathbf{B}_{\text{eff}}(t)$ is simply the vector sum of $\mathbf{B}_1(t)$ and $\Delta\boldsymbol{\omega}(t)/\gamma$. Finally, we define one additional reference frame (x'', y'', z''), known as the B_{eff} frame (*11*), in which $\mathbf{B}_{\text{eff}}(t)$ remains collinear with the longitudinal axis (z'').

The FM frame (Fig. 1a) can be transformed to the B_{eff} frame (Fig. 1b) by the rotation operator $\exp[-i\alpha(t)I_y]$. For an AFP pulse, the total sweep angle α_{tot} is 180°; thus, a 180° rotation about $y' = y''$ describes the final relative orientation between FM and B_{eff} frames. In the B_{eff} frame, the effective field $\mathbf{E}(t)$ is the vector sum of the fields, $[(d\alpha/dt)/\gamma]\hat{\mathbf{y}}''$ and $B_{\text{eff}}(t)\hat{\mathbf{z}}''$. As Fig. 1b illustrates, the initial transverse magnetization $\mathbf{M}$ rotates about $\mathbf{E}(t)$ in a plane that is related to the $x''y''$ plane by a rotation about x'' given by

$$\theta(t) = \arctan\left[\frac{(d\alpha/dt)}{\gamma B_{\text{eff}}(t)}\right]. \qquad [2]$$

If $|\gamma B_{\text{eff}}(t)| \gg |d\alpha/dt|$ for all t (i.e., when the adiabatic condition is satisfied throughout the pulse), $\theta \approx 0$ and $\mathbf{M}$ simply rotates about $\mathbf{B}_{\text{eff}}$ through a phase angle ψ given by

1090-7807/97 $25.00

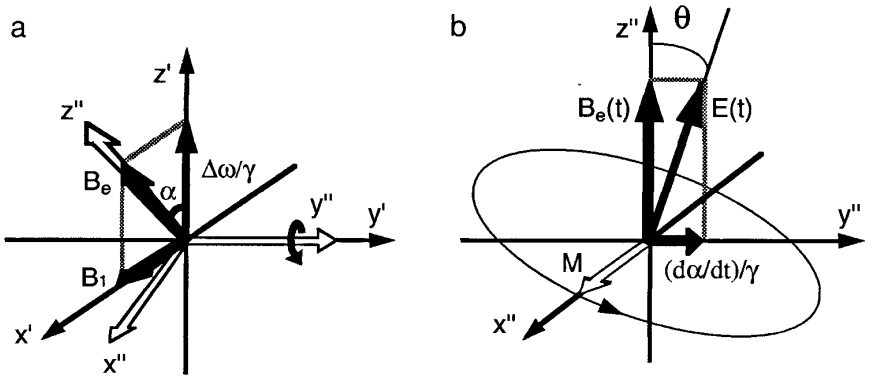

FIG. 1. (a) Relationship between the frequency-modulated (FM) frame (x', y', z') and the B_{eff} frame (x'', y'', z''), showing the rotation angle α in a classical adiabatic experiment. (b) Magnetic fields and motion of the magnetization vector **M** about the resultant magnetic field **E** in the B_{eff} frame.

$$\psi(t) \approx \gamma \int_0^t \mathbf{B}_{\text{eff}}(t')dt'. \qquad [3]$$

The total accumulated phase ψ_{tot} (Eq. [3]) varies with chemical shift, since $\Delta\omega(t)$, and thus $B_{eff}(t)$, depend on resonance offset (Eq. [1]).

This chemical-shift dependence can be eliminated with a sequence of AFP pulses separated by one or more B_{eff} flips, which reverse the direction of spin precession so that $\psi_{tot} = 0$. To attain constant-phase refocusing with this approach, two criteria must be satisfied (*5*). First, in the B_{eff} frame, the spin vectors must undergo an identity transformation, which is achieved by a *proper* combination of AFP pulses separated by instantaneous B_{eff} flips. Second, to achieve a flip angle of 180° by the end of the pulse, the B_{eff} frame must undergo a 180° rotation with respect to the FM frame. When the individual adiabatic segments between the B_{eff} flips are AFP pulses, the total flip angle is simply the sum of the sweep angles (α_{tot}) of the B_{eff} trajectories, and therefore, an odd number of AFP segments must be employed to achieve refocusing.

Recent reports by Kupče and Freeman (*20*) and by Tannus and Garwood (*21*) show a new procedure to construct AFP pulses with offset-independent adiabaticity, which ensures uniform inversion within the frequency limits of the adiabatic sweep. For this kind of pulse, the appropriate frequency-modulation function is obtained by taking the time integral of the square of its amplitude-modulation function. The well-known hyperbolic secant (HS) pulse (*1, 2*) is an example of an AFP pulse that achieves offset-independent adiabaticity. The driving function for the frequency modulation in the HS pulse can be derived from its amplitude-modulation function, sech($\beta\tau$), by (*20, 21*)

$$F_2(\tau) = \int_0^\tau \text{sech}^2(\beta\tau')d\tau' = \frac{\tanh(\beta\tau)}{\tanh(\beta)}, \qquad [4]$$

where $\tau(=2t/T_p)$ is defined in the interval $-1 \leqslant \tau \leqslant 1$, and the truncation factor β is chosen such that sech(β) = 0.01.

One way to reduce the peak power of the HS pulse is to raise the time variable in the sech function to a higher power. For example, when the time variable is raised to its 8th power, the corresponding frequency-modulation function is then (*21*)

$$F_2(\tau) = \int_0^\tau \text{sech}^2(\beta\tau'^8)d\tau'. \qquad [5]$$

This pulse has been dubbed HS8. In order to apply these shaped pulses in current spectrometers equipped with waveform generators, the corresponding phase-modulation functions are obtained by integrating the frequency-modulation functions with respect to time either analytically or numerically (*20, 21*). To characterize the relation between the bandwidth and pulse length of individual as well as composite adiabatic pulses, a convenient unitless parameter R is often used (*22, 23*)

$$R = A \cdot T_p/\pi = \text{bw} \cdot T_p, \qquad [6]$$

where bw is the pulse bandwidth in hertz and T_p is the pulse length in seconds. We will use HS and HS8 pulses with different R values to construct adiabatic refocusing pulses. These principles can be applied to all types of adiabatic inversion pulses used for refocusing purposes, and the R values of these pulses can be easily changed for different applications.

Figure 2 shows timing diagrams of adiabatic refocusing pulses of total pulse length T_p composed of different AFP pulses with B_{eff} flips between segments. The specific sequence in Fig. 2a, [HS (R = 25), HS (R = 50), HS (R = 25)], was used to acquire the experimental data in Fig. 3. The HS pulse lengths are adjusted proportionally with R to have the same bandwidth for each pulse. The following nomenclature is used to define this class of composite adiabatic pulses: [the name of the AFP pulse (e.g., HS), followed by the sequence of R values describing the individual

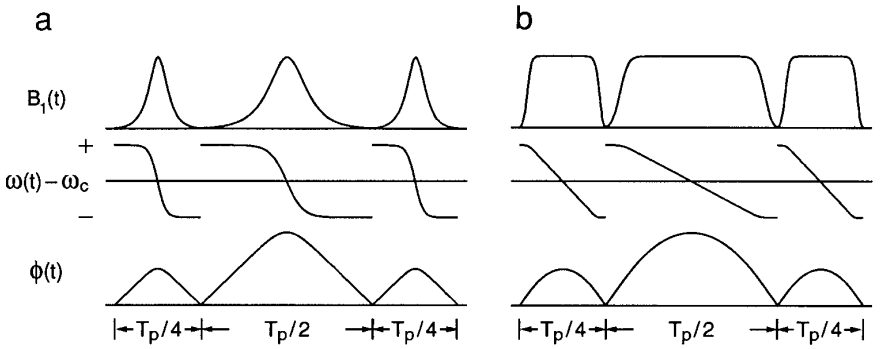

FIG. 2. Timing diagram of the 3π adiabatic refocusing pulses for (a) [HS-25, 50, 25] and (b) [HS8-50, 100, 50]. $B_1(t)$, $\omega(t)$-ω_c, and $\phi(t)$ represent the shapes of their amplitude-modulation function, frequency-modulation function, and phase-modulation function, respectively. T_p is the total pulse length.

AFP segments]. Accordingly, the sequence above can be written as [HS-25, 50, 25]. During this pulse, B_{eff} flips occur between adjacent HS pulses. In the case where the adiabatic condition is satisfied, complete refocusing of spins in the B_{eff} frame (Fig. 1b) can be examined by calculating whether $\int_0^{T_p} \mathbf{B}_{\text{eff}}(t) = 0$.

It can be shown that

$$\psi_{\text{tot}} = \gamma\left[\int_0^{0.25T_p} B_{\text{eff}}(t)dt - \int_{0.25T_p}^{0.75T_p} B_{\text{eff}}(t)dt + \int_{0.75T_p}^{T_p} B_{\text{eff}}(t)dt\right] = 0, \quad [7]$$

when the ratio of R values for the constituent pulses is 1:2:1. For pulses of this type, the B_{eff} frame experiences a net 180° rotation relative to the FM frame, and thus, phase-compensated refocusing takes place over a bandwidth roughly equal to the frequency sweep range. Constructing adiabatic refocusing pulses in a time-symmetric manner, such as [HS-25, 50, 25], leads to a symmetric frequency profile, independent of the sign of resonance offsets (*24*), and opens more possibilities of concatenating adiabatic pulses, provided that the number of AFP pulses is odd so that a net 180° rotation is achieved and that the sum of the R values of the odd-numbered AFP pulses in the sequence equals the sum of the R values of the even-numbered AFP pulses. For example, five consecutive AFP pulses with the R ratios 2:3:2:3:2 will also refocus spins with complete phase compensation. These properties make the time-symmetric refocusing pulses intrinsically different from the 3π pulse proposed in Ref. (*18*).

Spectra were acquired using a Varian Unity*plus* 500 MHz spectrometer equipped with triple-resonance PFG probe, RF waveform generator, and shielded z-gradient unit. The sample was 1% H_2O in D_2O, doped with 0.1 mg/ml $GdCl_3$. Interscan delay was 3 s. To avoid phase problems induced by transmitter jumps between different offsets, resonance offsets were created by adding a phase ramp to the original phase-modulation function. All spectra were acquired by a *single*-scan spin-echo sequence in which the 180° pulse is surrounded by a gradient pair. The on-resonance spectrum was phased to absorption mode, and this phase correction was applied to the other traces.

Figure 3 compares the refocusing profiles of a hard 180° pulse (Fig. 3a), a broadband composite pulse (*26*) (Fig. 3b), and [HS-25, 50, 25] (Fig. 3c). The $\gamma B_1^{\max}$ level used was 9.80 kHz (γB_1^{rms} = 4.26 kHz for the HS pulses). For any kind of refocusing pulse in a spin-echo sequence, the transformation of magnetization can be written as (*15*)

$$\begin{bmatrix} M_x \\ M_y \\ M_z \end{bmatrix} = \begin{bmatrix} P\cos(2\delta) & P\sin(2\delta) & 0 \\ P\sin(2\delta) & -P\cos(2\delta) & 0 \\ 0 & 0 & 1-2P \end{bmatrix} \times \begin{bmatrix} m_x \\ m_y \\ m_z \end{bmatrix}, \quad [8]$$

where P indicates how much the spin is flipped by the refocusing pulse, and can be calculated according to (*15, 25*)

$$P = \frac{1}{2}\left(1 - \frac{M_z}{m_z}\right). \quad [9]$$

The 2δ phase shift can be understood as a result of a 180° rotation about the transverse component of the *net* rotation axis for the refocusing pulse. For adiabatic refocusing pulses proposed in this Communication, $2\delta = \psi_{\text{tot}}$ within the working bandwidth, provided that $\theta = 0$ in Fig. 1b. With both the hard pulse and the broadband composite hard pulse, the rotation axes are contained in the $x'z'$ plane (*26*), which

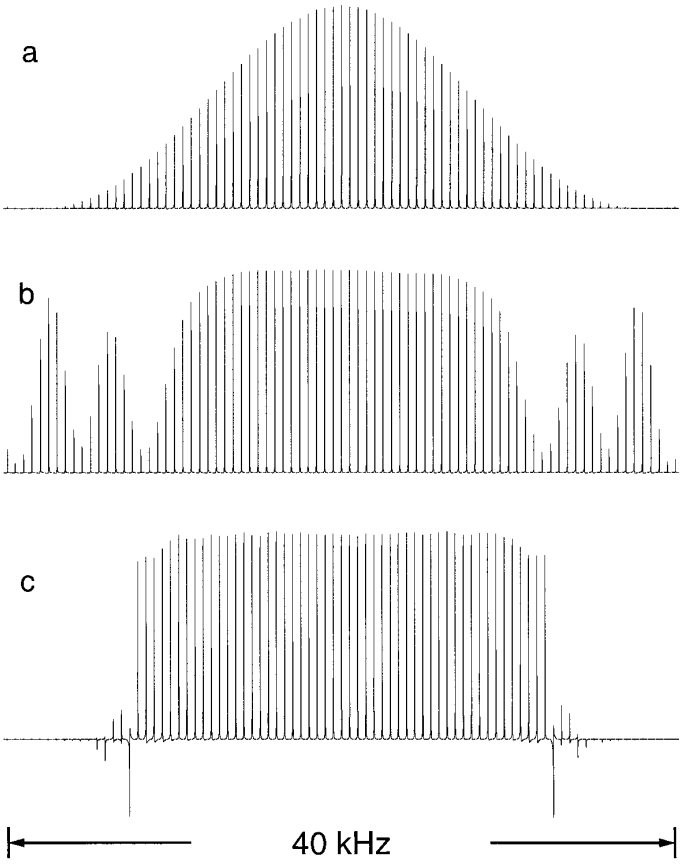

FIG. 3. Symmetric refocusing profiles of (a) a hard 180° pulse, (b) the broadband constant 180° rotation pulse (*26*), $27^\circ_x\ 99^\circ_{-x}\ 180^\circ_x\ 211^\circ_{-x}\ 386^\circ_x\ 211^\circ_{-x}\ 180^\circ_x\ 99^\circ_{-x}\ 27^\circ_x$, and (c) the [HS-25, 50, 25] with 4 ms duration, all obtained at $\gamma B_1^{\max} = 9.8$ kHz. The resonance offsets were stepped from −20 to 20 kHz in increments of 500 Hz.

ensures that $\delta = 0$ and no phase roll occurs across the spectrum.

Although the refocusing profile of the broadband composite hard pulse is wider than the hard 180° pulse, its performance is sensitive to B_1 inhomogeneity (*26*). This situation also applies to other broadband symmetric composite hard pulses for 180° rotation (*27*). However, since [HS-25, 50, 25] is composed of three adiabatic pulses, the performance is insensitive to B_1 inhomogeneity when the adiabatic condition is satisfied. From the positions of the net rotation axes of the 3π refocusing pulse at different resonance offsets, we can also understand why it works. Outside the working bandwidth ($|\Omega| > A$), the 3π pulse performs a z rotation as a single HS pulse does, leading to P roughly equal to zero. However, upon passing the transition regions ($|\Omega| \leqslant A$), the projection of rotation axis onto the y' direction increases rapidly from 96% to more than 99% of the maximum. Hence, the 2δ phase shifts are approximately constant within the 25 kHz refocusing bandwidth. We calculated, at different resonance offsets, the probability P for the intensity of refocused magnetization, and the phase difference relative to the spectrum on resonance for [HS-25, 50, 25] using experimental parameters. The simulation result agrees very well with the experimental data shown in Fig. 3c.

To further demonstrate the principle, the refocusing pulse [HS8-50, 100, 50] was generated. First, T_p was set to 3 ms (i.e., the lengths of the three consecutive AFP pulses were 0.75, 1.5, and 0.75 ms, respectively), and $\gamma B_1^{\max}$ was 8460 Hz ($\gamma B_1^{\text{rms}} = 7530$ Hz). This pulse achieved refocusing across a bandwidth roughly equal to 60 kHz as shown in Fig. 4a. When the total pulse length T_p was reset to 1 ms and $\gamma B_1^{\max}$ was raised to 25,570 Hz ($\gamma B_1^{\text{rms}} = 22{,}760$ Hz), the refocusing bandwidth was roughly 172 kHz (Fig. 4b). Note that when the pulse length was reduced by $\frac{1}{3}$, the required $\gamma B_1^{\max}$ (or γB_1^{rms}) and the refocusing bandwidth increased threefold. This proportionality, also suitable for other kinds of adiabatic refocusing (inversion) pulses, can be applied to determine the peak $\gamma B_1^{\max}$ level for different bandwidths. When comparing the above results with double-echo experiments employing two HS8 ($R = 100$) pulses with 1.5 ms ($\gamma B_1^{\max} = 8460$ Hz) or with 0.5 ms ($\gamma B_1^{\max} = 25570$ Hz), the refocusing bandwidths are very similar. If two HS8 ($R = 50$) pulses with 0.75 or 0.25 ms were used for double-echo experiments, slightly higher $\gamma B_1^{\max}$ values were required to reach uniform refocusing in the working bandwidths.

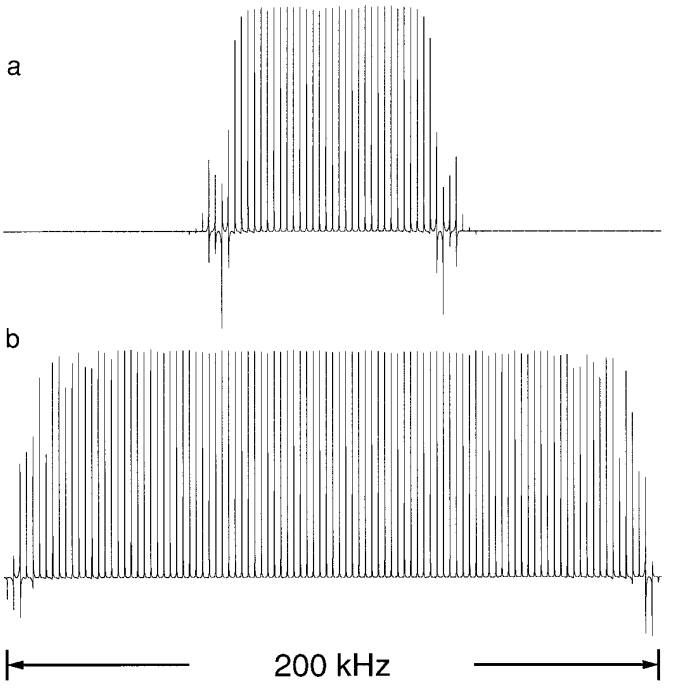

FIG. 4. Symmetric refocusing profiles acquired by using (a) [HS8-50, 100, 50] with 3 ms duration and $\gamma B_1^{\max} = 8460$ Hz ($\gamma B_1^{\text{rms}} = 7530$ Hz), and (b) [HS8-50, 100, 50] with 1 ms duration and $\gamma B_1^{\max} = 25570$ Hz ($\gamma B_1^{\text{rms}} = 22760$ Hz). The resonance offsets were stepped from −100 to 100 kHz in increments of 2 kHz.

In conclusion, we have shown an approach to construct time-symmetric adiabatic refocusing pulses with no appreciable phase distortion within the working bandwidth. This approach is applicable to different kinds of adiabatic inversion pulses (*20, 21*) for refocusing practice. Although this type of adiabatic refocusing pulses deposits higher heating to the sample as compared to a single inversion pulse, this is not expected to be a significant limitation for high-resolution NMR, because its contribution to the duty cycle is negligible at the predelays commonly used in high-resolution NMR.

ACKNOWLEDGMENTS

The authors thank Dr. Alberto Tannus for helpful discussions. This research was supported by NIH Grants RR11115 (P.v.Z., T.L.H.), and RR08079 and CA64338 (M.G.).

REFERENCES

1. J. Baum, R. Tycko, and A. Pines, *Phys. Rev. A* **32,** 3435 (1985).
2. M. S. Silver, R. I. Joseph, and D. I. Hoult, *J. Magn. Reson.* **59,** 347 (1984).
3. M. R. Bendall, M. Garwood, K. Ugurbil, and D. Pegg, *Magn. Reson. Med.* **4,** 493 (1987).
4. M. Garwood, and Y. Ke, *J. Magn. Reson.* **94,** 511 (1991).
5. M. Garwood, and K. Ugurbil, *in* ''NMR Basic Principles and Progress'' (M. Rudin and J. Seelig, Eds), p. 109, Springer-Verlag, New York, 1992.
6. M. R. Bendall, *J. Magn. Reson. A* **112,** 126 (1995).
7. Ē. Kupče, and R. Freeman, *J. Magn. Reson. A* **115,** 273 (1995).
8. R. Fu, and G. Bodenhausen, *J. Magn. Reson. A* **117,** 324 (1995).
9. M. Garwood, B. Nease, Y. Ke, R. A. de Graaf, and H. Merkle, *J. Magn. Reson. A* **112,** 272 (1995).
10. P. C. M. van Zijl, T.-L. Hwang, M. O'Neil Johnson, and M. Garwood, *J. Am. Chem. Soc.* **118,** 5510 (1996).
11. K. Ugurbil, M. Garwood, A. R. Rath, and M. R. Bendall, *J. Magn. Reson.* **78,** 472 (1988).
12. K. Hallenga, and G. M. Lippens, *J. Biomol. NMR* **5,** 59 (1995).
13. M. H. Levitt, and R. Freeman, *J. Magn. Reson.* **43,** 65 (1981).
14. S. Conolly, G. Glover, D. Nishimura, and A. Macovski, *Magn. Reson. Med.* **18,** 28 (1991).
15. T.-L. Hwang, and A. J. Shaka, *J. Magn. Reson. A* **112,** 275 (1995).
16. V. L. Ermakov, J.-M. Bohlen, and G. Bodenhausen, *J. Magn. Reson. A* **103,** 226 (1993).
17. C. S. Poon, and R. M. Henkelman, *J. Magn. Reson. A* **116,** 161 (1995).
18. S. Conolly, D. Nishimura, and A. Macovski, *J. Magn. Reson.* **83,** 324 (1989).
19. M. Nuss, D. Whittern, and M. Garwood, *in* ''Works in Progress, Society of Magnetic Resonance in Medicine, Ninth Annual Meeting,'' New York, p. 1298, 1990.
20. Ē. Kupče and R. Freeman, *J. Magn. Reson. A* **118,** 299 (1996).
21. A. Tannus and M. Garwood, *J. Magn. Reson. A* **120,** 133 (1996).
22. Y. Ke, D. G. Schupp, and M. Garwood, *J. Magn. Reson.* **96,** 663 (1992).
23. T.-L. Hwang, M. Garwood, A. Tannus, and P. C. M. van Zijl, *J. Magn. Reson. A* **121,** 221 (1996).
24. M. H. Levvit, *J. Magn. Reson.* **48,** 234 (1982).
25. A. J. Shaka and R. Freeman, *J. Magn. Reson.* **63,** 596 (1985).
26. A. J. Shaka and A. Pines, *J. Magn. Reson.* **71,** 495 (1987).
27. D. Abramovich and S. Vega, *J. Magn. Reson. A* **105,** 30 (1993).